ORIGINAL PAPER

JMS Journal of Medical Science

A simple model of human walking

Leonardo Campanelli
All Saints University School of Medicine, Toronto, Canada
–
Corresponding author: leonardo.s.campanelli@gmail.com

DOI: https://doi.org/10.20883/medical.e817

Keywords: human locomotion, gait, inverted pendulum model, modelling

Received: 2023-02-10
Accepted: 2023-03-01
Published: 2023-03-01

How to Cite: Campanelli L. A simple model of human walking. Journal of Medical Science. 2023;92(1);e568. doi:10.20883/medical.e817

ABSTRACT

Aim. We investigate Alexander's inverted pendulum model, the simplest mathematical model of human walking. Although it successfully explains some kinematic features of human walking, such as the velocity of the body's centre of mass, it does not account for others, like the vertical reaction force and the maximum walking speed. This paper aims to minimally extend Alexander's model in such a way as to make it a viable and quantitative model of human walking for clinical biomechanics.
Material and methods. In order to compare the predictions of Alexander's model with experimental data on walking, we incorporate in it a robust phenomenological relation between stride frequency and stride length derived in the literature, and we introduce a step-angle dependent muscle force along the pendulum. We then analytically solve the pendulum's motion equation and find the corresponding analytical expression for the average walking speed.
Results. The values of the average walking speed for different heights predicted by our model are in excellent agreement with the ones obtained in treadmill experiments. Moreover, it successfully predicts the observed walking-running transition speed, which occurs when the stride length equals the height of an individual. Finally, our extended model satisfactorily reproduces the experimentally observed ground reaction forces in the midstance and terminal stance phases. Consequently, the predicted value of the (height-dependent) maximum walking speed is in reasonable agreement with the one obtained in more sophisticated models of human walking.
Conclusions. Augmented with our minimal extensions, Alexander's model becomes an effective and realistic model of human walking applicable in clinical investigations of the human gate.

1. Introduction

The physics and mathematics of animal locomotion are fundamental in several disciplines. For example, biomechanical models can allow paleobiologists to deduce the main characteristics of the locomotion of extinct animals from their fossilized remains (see [1]). In athletics, mathematical models of human locomotion can attempt to determine the theoretical optimum performance in certain events such as race walking (see [2]). However, medical engineers and clinical biomechanists are instead concerned with animal locomotion because of its relevance to determining limb and joint forces, which play a crucial role in rehabilitation from either injury or disease (see [3]).

Human walking is one of the simplest gaits of terrestrial locomotion among legged animals. Nevertheless, a clear and definitive understanding of the energetics, stability, and kinematics still needs to be included (for a review of analytical modelling and experimental studies of human walking, see [4]).

Theoretical and experimental works on human walking have focussed on energetics and stability or kinematics. In the former case, mechanical energy principles are applied to relate the mass-specific metabolic energetic cost and mechanical cost of transport to the dynamical properties of gait (see [5–7]). In the latter case, which is more relevant to clinical biomechanics, Newtonian dynamical equations applied to simple inertial models of jointed rigid bodies are used to determine the motion of the components during walking (see [8]).

The simplest model of human walking is the two-dimensional "Alexander's inverted pendulum (IP) model" [9], which consists of a simple inverted pendulum where the whole body mass concentrates in a single particle. It was introduced in the late 70s, although probably, the first indirect references to an inverted pendulum as a model of human walking date back to 1953 [10]. In recent years, a great variety of two-dimensional kinetic models based on the IP model have been developed to mimic better and understand the pattern of human walking.. These models include springs [11–16], dampers [17], and additional segments and joints, or either additional segments or joints [18, 19] (for other works based on the IP model, see [20–24]).

The apparent limitation of two-dimensional models of human walking is that they are unable to describe the lateral dynamics of the gait. Such dynamics can only be studied by more sophisticated three-dimensional models, like those constructed in [25–29]. In particular, the vertical, horizontal, and lateral ground reaction forces (GRF) predicted by the recent three-dimensional bipedal model by Liang et al. [30] agree with experimental data.

Since the introduction of the IP model by Alexander, the level of complexity of walking models has increased, as the number of parameters needed to reproduce quantitatively and in a satisfactory way the characteristics of the human gate. Moreover, Alexander's model cannot describe the lateral motion and the transition from one step to another. On the other hand, its simplicity has attracted many authors' attention over the years (see [2, 18, 31, 32]) as the kinematics and dynamics of walking during the double support phase (where the transition from one step to another occurs) are not as crucial for clinical biomechanics as the kinematics and dynamics of walking in the single support phase. Also, the importance of lateral motion in clinical application is subdominant, at least at first approximation, for the vertical and horizontal ones. While Anderson and Pandy [31] briefly described the GRF in the IP model, Buczek et al. [32] performed a more detailed analysis and compared the prediction of the model about GRF and velocity of the center of mass with gait data for regular walking. This work was extended by McGrath et al. [18] by including fast and slow walking speeds, which are essential for clinical considerations (the inclusion of an actuated hip joint to the IP model, although engaging in that it reproduced the experimentally measured hip moment curve, did not resulted in significant changes in the kinematics of the centre of mass and ground reaction forces). These studies conclude that that, while the horizontal and vertical velocities of the centre of mass and the horizontal GRF in the midstance and terminal stance phases agree reasonably well with experimental data, the vertical component of the GRF does not, especially for fast walking.

One of the goals of this paper is to extend these works by including a step-angle-dependent muscle force along the IP in such a way as to reproduce the experimentally observed vertical GRFs in the single support phase. Also, we will show that Alexander's model successfully predicts the observed walking-running transition speed.

2. Methods and Results

2.1. The inverted pendulum model: Generalities

The human body, while walking, can be represented as an inverted pendulum with variable moment of inertia concerning the instantaneous axis of rotation subject to different (natural) forces and torques. Alternatively, one can assume a constant moment of inertia and regard the telescopic actions of the body (principally due to the

swinging limbs) as generating inertial forces and torques.

In this latter case, the scalar projection along the instantaneous axis of rotation of the equation of motion $\dot{\mathbf{L}} = \boldsymbol{\tau}_{\text{net}}^{(\text{ext})}$, $\mathbf{L}$ is the angular momentum, reads

$$I\ddot{\theta}(t) = \tau_{\text{net}}^{(\text{ext})}. \quad (1)$$

Here, I is the constant moment of inertia concerning the instantaneous axis of rotation y (see **Figure 1**),

$$\boldsymbol{\tau}_{\text{net}}^{(\text{ext})} = \boldsymbol{\tau}_g + \boldsymbol{\tau}_{\text{int}} \quad (2)$$

is the net external torque, τ_g is the gravitational torque, and τ_{int} is the body-ground interaction torque generated by the muscle forces and includes all telescopic actions. Also, a dot denotes differentiation regarding time, and θ is the angle formed by the pendulum and the vertical (the z-axis in **Figure 1**). Notice that θ is measured starting from the vertical and is negative (positive) on the left (right) of the z-axis.

In order to solve the above equation of motion, one has to know the exact expression of the (time-dependent) torques generated by the body muscles during the entire gait cycle.

It is important to observe, however, that the kinematics (horizontal and vertical velocities of the centre of mass) and dynamics (ground reaction forces) of walking are experimentally symmetrical concerning the vertical, at least in the first approximation [4] and especially for slow and regular walking allowing us to focus our analysis on the phase of the gait cycle that goes from the double-support phase to the vertical. Moreover, roughly speaking, the effect of the first part of the propulsion force is impulsive, with the propulsion force provided by the gluteus maximus of the supporting leg and by the swinging of the opposite leg. In contrast, the second part of the propulsion spreads out more temporally and is provided essentially by the gastrocnemius [33]. However, the centre of mass of the gastrocnemius, and then the point of application of the force generated by it, is situated below the knee so that its contribution to the interaction torque is reduced concerning that given by the gluteus maximus, whose point of application is near to the centre of mass of the body. In the first approximation, the interaction torque generated by the gastrocnemius can be neglected. Accordingly, the gluteus maximus and the swing-

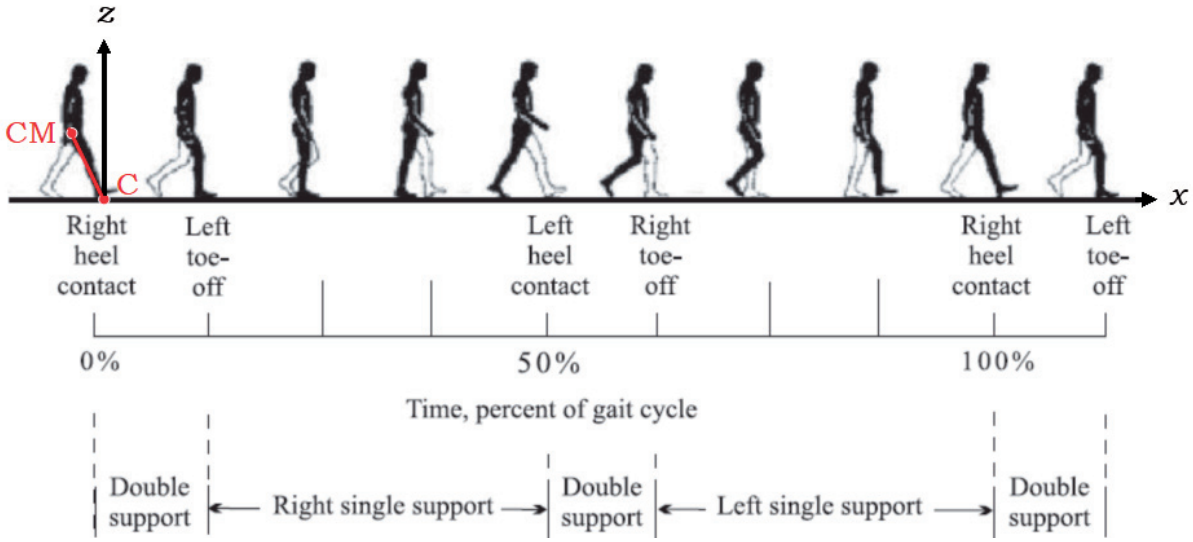

Figure 1. Schematic view of human walking during a gait cycle (adapted from [4]). In the stiff-leg approximation, the trajectory of the centre of mass of the walker (point CM) is an arc of a circle whose centre is the point of contact body-ground (point C). The angle between the (stiff) leg and the vertical axis is the "step angle" θ. In the inverted pendulum model of human walking, θ coincides with the angle formed by the z-axis and the line connecting CM and the fixed point C. In the model discussed below, the muscle force $\mathrm{F}_{\text{muscle}}$ is directed along the leg. Notice that in the text and following [18], we will assume the duration of the double support phase to be 10% of the gait cycle and that the supporting leg reaches the vertical position at 30% of the gait cycle.

ing of the opposite leg, principally during the second part of the double support phase, provide the only propulsion force.

As already noticed, Alexander's model cannot describe the transition from one step to another during the double support phase. Thus, its application must be limited to the single support phase. In this phase, which is the most important one in clinical studies, the interaction torque is negligible, and the gravitational force ultimately determines the dynamics of the inverted pendulum.

Referring to **Figure 1**, the gravitational torque is given by

$$\boldsymbol{\tau}_g = -mgr_{\mathrm{cm}} \sin\theta \tag{3}$$

where m is the mass of the body, g = 9.8m/s^2 is the acceleration of gravity, r_{cm} is the distance between the fixed point and the centre of mass of the body, and **j** is the unit vector along the y-axis (the body is moving in the positive x-direction).

The solution of Eq. (1) in the single support phase will be discussed in Sec. 2.4. In the rest of this section, we introduce some physical quantities significant for the following discussions about the kinematics and dynamics of Alexander's model.

The moment of inertia I can be written as

$$I = \delta m r_{\mathrm{cm}}^2 \tag{4}$$

where δ is a dimensionless parameter. The value $\delta = 1$, which will be used throughout this paper, corresponds to the simple case where all the body mass concentrates in the centre of mass (simple inverted pendulum). Moreover, we write

$$r_{\mathrm{cm}} = \sigma h \tag{5}$$

where σ is a dimensionless parameter and h is the body height. Henceforth, we will use the value σ = 0.56, corresponding to an erect person with arms at the side [34]. The period of the IP oscillation (equal to the stride time) can be written as

$$t_s = 2\pi\sqrt{\frac{h}{\xi g}}, \tag{6}$$

where ξ is a dimensionless parameter that generally depends on the initial step angle θ_0.

2.2. Average speed of walking

Two fundamental parameters in human gait are the stride frequency $f_s = 1/t_s$ and stride length L_s. Although it has been shown that they have distinct effects on gait variability, a strong positive linear correlation has been found between them in free walking [35],

$$L_s = af_s + b, \tag{7}$$

where $a \simeq 1.7$ and $b \simeq -0.30$. The analysis in [35] was performed on individuals of an average height of $h = 1.65$m. Inserting Eq. (7) into Eq. (6) and solving for ξ, we find

$$\xi = \frac{1}{g}\left(\frac{2\pi}{a}\right)^2 (4\sigma h \sin|\theta_0| - b)^2, \tag{8}$$

where we used Eqs. (5) and (6). As a working hypothesis, let us assume ξ to be independent of the height of a person (this *ansatz* is justified *a posteriori* in that the speed of walking predicted by the IP model agrees well, as we will show, with the experimental data from individuals of very different heights). In this case, a and b scale as $a \propto h^{3/2}$ and $b \propto h$, respectively. Writing $a = a_0 h^{3/2}$ and $b = b_0 h$, we then have

$$\xi = \frac{1}{g}\left(\frac{2\pi}{a_0}\right)^2 (4\sigma \sin|\theta_0| - b_0)^2, \tag{9}$$

where $a_0 = 0.80$ and $b_0 = -0.18$, or

$$\xi(s) = 0.207 + 2.28s + 6.26s^2, \tag{10}$$

where we have defined

$$s = \frac{L_s}{h} = 4\sigma \sin|\theta_0|. \tag{11}$$

Let us now calculate the average walking speed, defined as the horizontal component of the velocity of the centre of mass, averaged over the stride time. In our case, this corresponds to $\overline{v_x} = L_s/t_s$, so that

$$\overline{v_x} = \frac{s}{2\pi}\sqrt{\xi(s) g h}. \tag{12}$$

Notice that the results in [35] are valid for walking speeds between 0.75m/s and 1.80m/s for a height of 1.65m, which means that the expression for $\xi(s)$ can be trusted when the initial step angle is in the interval $0.27 \lesssim |\theta_0| \lesssim 0.45$ (this

Table 1. Physical characteristics (h, h_{leg}, and L_s/h), walking speed ($\overline{v_x}$), and Froude number (Fr) of the four stature-age groups analyzed in [5]. An asterisk indicates the prediction of the inverted pendulum model.

Group	h(m)	h_{leg} (m)	L_s/h	$\overline{v_x}$(m/s)	$\overline{v_x}$*(m/s)	Fr	Fr*
A	1.14 ± 0.02	0.58 ± 0.02	0.76 ± 0.03	0.96 ± 0.04	0.95 ± 0.07	0.16 ± 0.01	0.16 ± 0.02
B	1.42 ± 0.02	0.77 ± 0.02	0.76 ± 0.02	1.03 ± 0.03	1.06 ± 0.06	0.14 ± 0.01	0.15 ± 0.01
C	1.62 ± 0.01	0.86 ± 0.01	0.78 ± 0.02	1.13 ± 0.04	1.19 ± 0.06	0.15 ± 0.01	0.17 ± 0.02
D	1.77 ± 0.01	0.94 ± 0.01	0.76 ± 0.02	1.21 ± 0.04	1.19 ± 0.07	0.16 ± 0.01	0.15 ± 0.01

implies that Eq. (12) is valid for velocities between 0.78m/s and 1.88m/s for a height of 1.80m).

The step length is about 38% of a person's height during regular walking [5] ($s \simeq 0.76$), corresponding to a step angle of about $|\theta_0| \simeq 0.35$ (20°). For an "average individual" of height $h = 1.80$m, then, the average speed for regular walking is predicted to be around 1.2m/s (4.3km/h), in agreement with the experimental result of [5]. Equation (12) also returns walking speeds in good agreement with the ones experimentally measured in [5] and shown in **Table 1**. Here, h is the height, h_{leg} is the leg length, L_s/h is the ratio of the stride length to the height, $\overline{v_x}$ is the walking speed at the minimum measured metabolic cost of transport, and Fr is the Froude number for four different stature-age groups (named A, B, C, and D in [5]). In the sixth and eighth columns, we report the values of the average walking speed, $\overline{v_x}$*, and Froude number, Fr*, as predicted by the inverted pendulum model.

Iterestingly, the average walking speed is well approximated by the expression

$$\overline{v_x} \simeq 1.21\left(\frac{|\theta_0|}{20^\circ}\right)^{1.72}\left(\frac{h}{1.80\mathrm{m}}\right)^{1/2}\mathrm{m/s}. \qquad (13)$$

Notice that the maximum percentage deviation of the above-approximated expression from the exact one is less than 0.62% for $0.20 \leq |\theta_0| \leq 0.61$, namely well below the typical statistical error of about 4% in [5]. From Eq. (13), it follows that the average walking speed (given that a person's height is a fixed parameter) is controlled, in regular walking, only by the value of the initial step angle.

2.3. Walking-running transition

A spontaneous transition from walking to running is expected in humans at sufficiently high speeds (see [36–39]). Although in the past, such a transition was believed to occur in order to minimize the energetic cost of locomotion, it is now widely accepted that the ultimate reason for it has a physiological/kinematic origin: fatigue and discomfort in the tibialis anterior and other dorsiflexor muscles of the ankle are the triggers for the transition [40].

The walking-running transition can be kinematically described by the so-called Froude number $\mathrm{Fr} = v^2/gL$, where v and L are the typical speed and height of the hip joint from the ground of a moving animal, respectively [36]. In our case, we can define the Froude number as

$$\mathrm{Fr} = \frac{\overline{v_x}^2}{g h_{\mathrm{leg}}}, \qquad (14)$$

where h_{leg} is the leg length. From Eq. (12), and writing

$$h_{\mathrm{leg}} = \frac{h}{\rho}, \qquad (15)$$

we find

$$\mathrm{Fr} = \frac{\rho}{4\pi^2} s^2 \xi(s). \qquad (16)$$

For regular walking ($s \simeq 0.76$) and taking $\rho = 1.9$ [5], we find Fr ≃ 0.15, a value independent of an individual's height. This result agrees with the value experimentally determined in [5] for four different stature-age groups, as shown in **Table 1**.

It is believed that the preferred transition speed from walking to running takes place at a Froude number of about 0.5 [36]. In our model with $\rho = 1.9$, this value of Fr corresponds to $s = 1.0$ (and in turn to $|\theta_0| \simeq 0.46$ or $|\theta_0| \simeq 26.5^\circ$), i.e. the walking-running transition takes place, approximatively, when the stride length equals the height of the individual. For $s = 1$, the average walking speed at the walking-running transition is about $\overline{v_x} \simeq 1.9$m/s (6.9km/h) for a height of $h = 1.70$m, which is in excellent agreement with the results of Hreljac et al. [41] who found $\overline{v_x} = 1.88 \pm 0.11$m/s for 11 individuals with h = 1.70 ± 0.08m.

2.4. Kinematics: Horizontal and vertical velocities

Equation (1) describes the body's motion during the entire gait cycle. However, as discussed in Sec. 2.1, the interaction torque should be addressed during the single support phase. In this phase, then, the equation of motion reads

$$\theta'' = \sin\theta, \tag{17}$$

where we used Eqs. (2) and (3). Here, a prime denotes differentiation regarding t/t_0 and

$$t_0 = \sqrt{\frac{I}{mr_{\mathrm{cm}}g}} = \sqrt{\frac{\sigma\delta h}{g}}. \tag{18}$$

The solution of Eq. (17) with Dirichlet boundary conditions $\theta(0) = \theta_0$ and $\theta(t_s/t_0) = 0$ is easily found,

$$\theta(t) = -2\mathrm{am}(u|\mu), \tag{19}$$

where $\mathrm{am}(u \vee \mu)$ is the Jacobi amplitude for the Jacobi elliptic functions . Here,

$$u = \chi(1 - \frac{4t}{t_s}), \mu = -\frac{\pi^2}{4\sigma\delta\xi\chi^2}, \tag{20}$$

and x is implicitly defined by

$$\chi = F(-\frac{\theta_0}{2}|\mu), \tag{21}$$

where $F(\phi|\mu)$ is the elliptic integral of the first kind [42]. A graph of x as a function of $|\theta_0|$ for $\delta = 1$ and $\sigma = 0.56$ is given in **Figure 2**.

The angular speed $\omega(t) = \dot{\theta}(t)$ is

$$\omega(t) = \omega_f \mathrm{dn}(u|\mu), \tag{22}$$

where $\mathrm{dn}(u|\mu)$ is the Jacobi elliptic function of dn type and $\omega_f = \omega(t_s/4)$ is the angular speed at the vertical,

$$\omega_f = \frac{8\chi}{t_s}. \tag{23}$$

The horizontal and vertical components of the velocity of the centre of mass, v_x and v_z, are

$$v_x(t) = \omega\cos\theta, v_z(t) = -\omega\sin\theta. \tag{24}$$

They are shown in **Figure 3** as a function of time (expressed as a percentage of the gait cycle) for three different walking speeds. Following [18], we present data and our results for half of the gait cycle, from the middle of one double support phase (at 5% of the gait cycle) to the middle of the next (at 55% of the gait cycle). The dashed lines are the one-standard-deviation experimental data from Winter [43, 44], which refer to a person of height h = 1.80m. In contrast, the continuous ones are the predictions of the inverted pendulum model. Finally, **Table 2** describes the best-fit values for the fitted parameter θ_0 and the corresponding average speeds of walking. The left vertical continuous line indicates the end of one double support phase at 10% of the gait cycle, while the right one is the beginning of the next double support phase at 50%.

As it is clear from the figure, the horizontal velocities predicted by the IP model fit very well the experimental data, from slow to fast walking and on the entire gait cycle. The vertical ones, however, agree only in the midstance and terminal stance phases, whose boundaries are indicated by the two dotted vertical lines. Roughly speaking, the start of the midstance is at 15% of

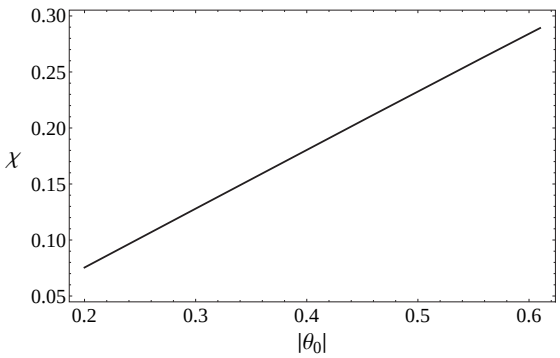

Figure 2. The function $x(\theta_0)$, implicitly defined by Eq. (21), for δ = 1 and σ = 0.56.

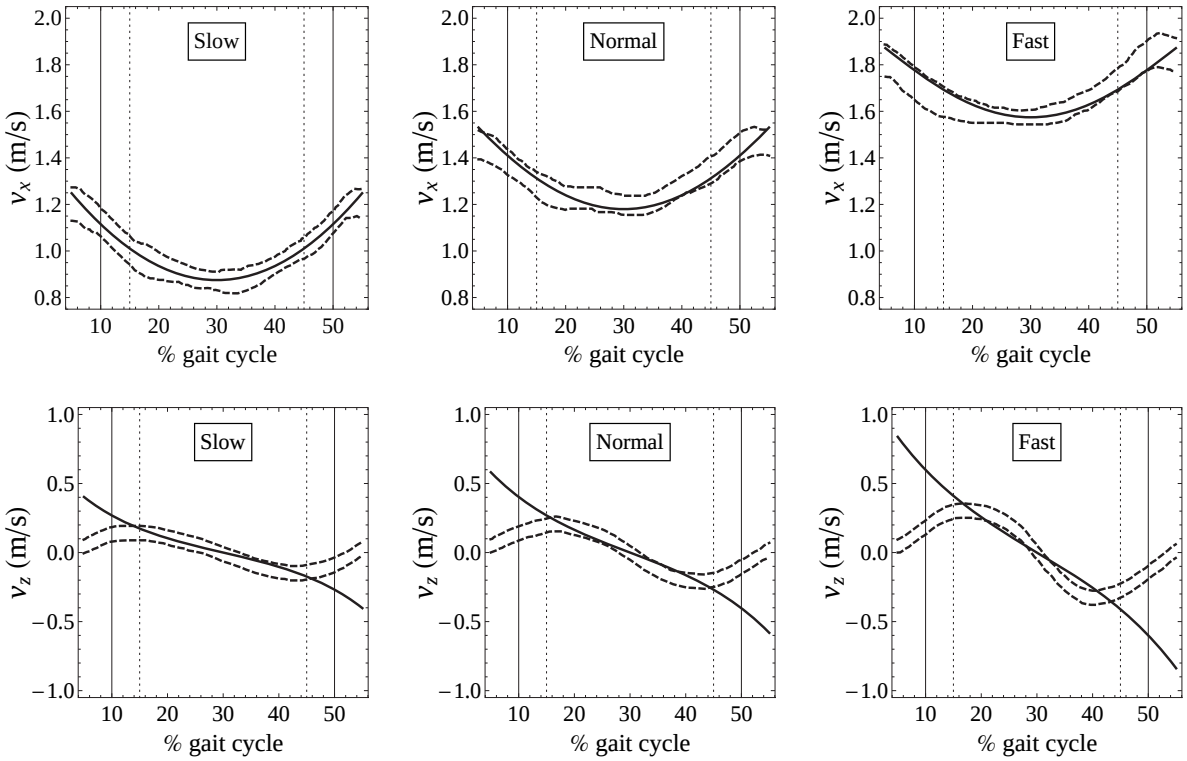

Figure 3. The horizontal (v_x) and vertical (v_z) components of the velocity of the centre of mass in the inverted pendulum model of human walking as a function of time (expressed as a percentage of the gait cycle) for three different walking speeds from the middle of one double support phase (at 5% of the gait cycle) to the middle of the next (at 55% of the gait cycle). The dashed lines are the one-standard-deviation experimental data from Winter [43, 44], while the continuous ones are the (best-fit) predictions of the inverted pendulum model. The left vertical continuous line indicates the end of one double support phase at 10% of the gait cycle, while the right one is the beginning of the next double support phase at 50%. The midstance phase extends from 15% of the gait cycle (left dotted vertical line) to the vertical (30% of the gait cycle). The terminal stance phase starts at the vertical and ends at 45% of the gait cycle (right dotted vertical line).

Table 2. Best-fit values of the initial step angle θ_0 for the three gaits depicted in **Figure 3** and the corresponding average walking speeds. Also indicated are the best-fit values of the coefficients a_n of the quartic polynomial in Eq. (28).

Gait	$\lvert\theta_0\rvert$	$\overline{v_x}$(m/s)	a_0	a_1	a_2	a_3	a_4
Slow	0.312	1.00	−0.0559	0.286	9.63	−6.73	−122
Normal	0.363	1.30	−0.126	0.00350	13.9	−0.303	−102
Fast	0.421	1.68	−0.193	0.0102	17.6	−2.82	−86.8

the gait cycle (left dotted vertical line), and the end of the terminal stance is at 45% (right dotted vertical line) [4].

2.5. Dynamics: Ground reaction forces

In Alexander's IP model of human walking, the vertical (F_z) and horizontal (F_x) ground reaction forces are

$$\frac{F_z}{mg} = (\cos\theta - t_0^2\omega^2)\cos\theta \qquad (25)$$

and

$$F_x = F_z\tan\theta, \qquad (26)$$

respectively. As a function of time and normalized to the body weight, these forces are shown in **Figure 4** by dot-dashed (grey) lines (the other notations are as in **Figure 3**).

As it is clear from the figure, while the predicted horizontal GRFs agree with the observed ones (especially in the single support phase), the vertical ones are not. The simple IP model cannot reproduce the characteristic "M" shape of the vertical GRF. Moreover, in the midstance and ter-

minal stance phases, the concavity of F_z is opposite to the one experimentally observed. Finally, Alexander's model predicts a maximum reaction at the vertical instead of the experimentally observed minimum.

The fact that the IP model does not account for the vertical force–time history can be explained by the omission, in the model, of the muscle forces (natural and inertial) generated by the body during the entire gait cycle, as explained in Sec. 2.1. On the other hand, the profile of the horizontal and vertical velocities of the centre of mass is well predicted by the model in the mid-stance and terminal stance phases, suggesting that in the single support phase, although active, they do indeed produce a little torque.

For this reason, and as a working hypothesis, let us introduce a time-dependent muscle force, F_{muscle}, directed along the pendulum (positive if pointing towards the fixed point, negative otherwise). The vertical reaction force becomes

$$\frac{F_z}{mg} = \left(\cos\theta - t_0^2\omega^2 + \frac{F_{\text{muscle}}}{mg}\right)\cos\theta\,, \qquad (27)$$

while the horizontal one is the same as in Eq. (26), with F_z replaced by the new expression (27).

Since the angle θ is generally small, we can expand F_{muscle} in terms of the step angle as

$$\frac{F_{\text{muscle}}}{mg} = \sum_{n=0}^{N} a_n \theta^n, \qquad (28)$$

where the coefficients a_n are, in general, functions of the initial step angle θ_0 (we will neglect a possible dependence of a_n on δ, σ, m, and h).

The continuous lines in **Figure 4** are the vertical and horizontal ground reaction forces when the muscle force is included. They were obtained by fitting the experimental data on the vertical reaction force by using Eq. (27). We found a good agreement with the data by truncating the expansion (28) to the fourth order (the inclusion of higher order terms did not improve the fit appreciably). **Table 2** depicts the values of the fitted parameters a_0, a_1, a_2, a_3 and a_4.

As it is clear from the figure, the introduction of a muscle force along the IP reproduces well

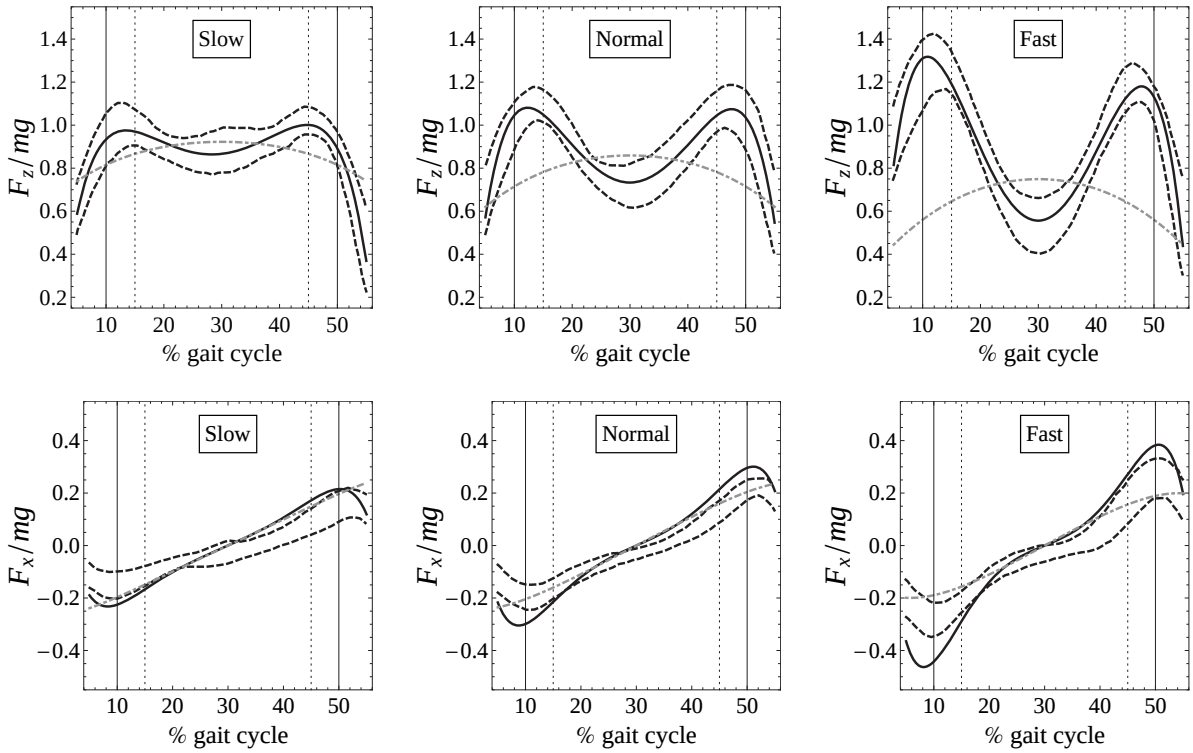

Figure 4. The horizontal (F_x) and vertical (F_z) ground reaction forces (normalized to the body weight mg) as a function of time (expressed as a percentage of the gait cycle) for three different walking speeds (the same of Figure 3). The dashed lines are the 1 standard-deviation experimental data from Winter [43, 44], while the dot-dashed (gray) lines are the prediction of the Alexander's IP model (with no muscle forces). The continuous lines are the (best-fit) predictions of the IP model with the inclusion of the muscle force (28). Vertical lines are as in **Figure 3**.

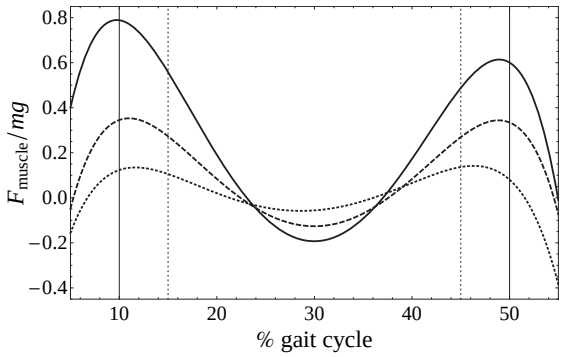

Figure 5. The muscle force in Eq. (28) (normalized to the body weight mg and for N = 4) as a function of time (expressed as a percentage of the gait cycle) for three different walking speeds: slow (dotted line), regular (dashed line), and fast (continuous line). The values of the expansion coefficients a_n and the corresponding average walking speeds for the three gaits are given in **Table 2**. Vertical lines are as in **Figure 3**.

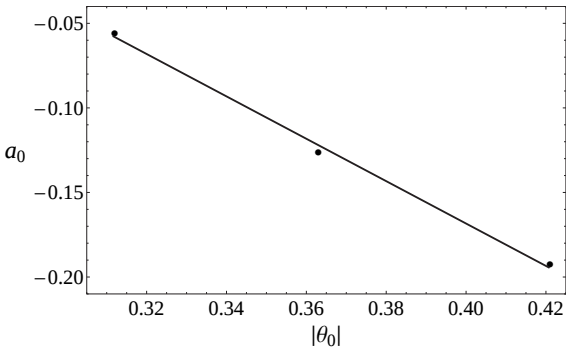

Figure 6. The parameter a_0 in Eq. (28) and **Table 2** as a function of $|\theta_0|$. The continuous line is the best-fitting line.

the vertical GRFs from slow to fast walking and in the entire gait cycle. The horizontal GRFs are satisfactorily reproduced only in the midstance and terminal stance phases.

Figure 5 shows the muscle force (28) that the body must generate to produce the ground reaction forces in **Figure 4** as a function of time. As discussed in Sec. 2.1, this force includes telescopic actions that could be, in principle, determined in more realistic and sophisticated models of human walking. However, it is plausible to assume that inertial forces are subdominant around the vertical compared to the ones generated by the gastrocnemius and the soleus [33]. These strong propulsive forces lift the heel and then are principally directed upward along the supporting leg, thus explaining the negative valley in the force-time diagram of **Figure 5**. The magnitude of these forces is crucial for the determination of the maximum speed of walking, as discussed in the next section.

2.6. Maximum speed of walking

In our simplified walking model, two conditions must be met to walk (for a general discussion of physical constraints during walking, see [45]). They are the condition of "no sliding" and the condition of "no-fly", the latter being violated when dynamical effects cause a "lifting" of the supporting foot (the point of contact body-ground). Assuming that the coefficient of static friction between the ground and the fixed point is sufficiently large to prevent sliding, the no-fly condition, $F_z > 0$, gives the value of the maximum initial step angle as the solution of the equation

$$t_0\omega_f = 1 + a_0. \tag{29}$$

The above equation can be solved if the explicit expression of a_0 as a function of the initial step angle is known (notice that a_0 is equal to the value of the muscle force per unit body weight at the vertical). An approximate expression for a_0 can be obtained by interpolating the three values of a_0 in **Table 2** for slow, regular, and fast walking. These values are shown in **Figure 6** together with the line of best-fit,

$$a_0 = 0.333 - 1.25|\theta_0|. \tag{30}$$

Inserting the above equation in Eq. (29) and solving for θ_0, we find the maximum initial step angle $|\theta_0|^{(\max)}$ = 0.61 (35°). This value is both outside the interpolation range (see **Table. 2**) and outside the range of θ_0 where the expression of $\xi(s)$ can be safely trusted (see discussion in Sec. 2.2). Interestingly enough, however, the corresponding value of the maximum speed of walking for a height of h = 1.75m, $\overline{v_x}^{(\max)} \simeq$ 3.1m/s (11km/h), agrees with the result of Marshall who found, by using a more sophisticate model of human walking, a maximal velocity between 2.7m/s and 3.3m/s (depending on the magnitude of the pelvic rotation).

3. Discussion

Alexander's model is the simplest model of human walking. If, on the one hand, its mathematical simplicity has attracted the attention of biomechanists, on the other hand, it results in two ineradicable limitations:

(*i*) It cannot describe the transition from one step to another, and, as for any two-dimensional model of human walking,

(*ii*) it cannot describe the lateral dynamics of the gait.

Moreover, it does not account for the temporal shape of the vertical reaction force and the maximum walking speed.

However, the mechanics of walking during the double support phase (where the transition from one step to another takes place) and the lateral motion are less important for clinical applications than the properties of the horizontal and vertical motions in the single support phase. For this reason, we added two new features to Alexander's model to make its predictions compatible with the observed vertical reaction force and the maximum walking speed.

First, we incorporated into the model a phenomenological relation between the stride frequency and stride length as determined in treadmill experiments. Second, we introduced a step-angle dependent force along the pendulum to simulate the effects generated during the single support phase by telescopic actions and propulsive muscle forces.

These minimal modifications make Alexander's model more physiologically representative and provide insight into the role of muscle forces during walking. In particular, we found that

(*i*) the experimental vertical reaction forces are fully reproduced by the extended model, as it is clear from the upper panels of **Figure 4**;

(*ii*) the muscle force at the vertical, primarily generated by the gastrocnemius and the soleus, critically contributes to the determination of the maximum speed of walking [see Eq. (29)];

(*iii*) the average speed of walking (see **Table 1**) and the walking-running transition speed (see the end of Sec. 2.3) agree with the ones found experimentally.

Finally, our extended Alexander's model is entirely solvable; indeed, we have provided an exact analytical solution to its equation of motion, which differs from the other extensions mentioned in the Introduction based on multiple pendulums, including springs and dampers. Unfortunately, in this case, the mechanics must be simplified to be analyzed analytically, and numerical methods must be used, resulting in a consequent loss of simplicity.

4. Conclusions

We have considered the two-dimensional inverted pendulum model of human walking, where the human body while walking, is approximated by a simple inverted pendulum. During a gait cycle and in the second part of the double support phase, propulsion torques are generated, which start the rotation of the inverted pendulum. Braking forces terminate such a rotation in the first part of the next double support phase. Although the pendulum model cannot describe such phases, it can reproduce the main characteristics of human gait in the single limb support phase, particularly in the midstance and terminal stance phases. To simplify our analysis, we have assumed that no propulsion/braking torques are active during the single limb support phase.

The main results of our paper are as follows.

(*i*) Using a phenomenological relation between stride frequency and stride length based on the literature, we have found an analytical expression for the average walking speed. The average speed is a function of only an individual's initial step angle and height. The predicted values of the average speed for different heights are in excellent agreement with the ones obtained in treadmill experiments.

Moreover, our expression for the average walking speed successfully predicts the observed walking-running transition speed, which, according to our results, occurs when the stride length equals the height of an individual.

(*ii*) We have found an exact analytical solution to the equation of motion of the two-dimensional inverted simple pendulum. Together with the phenomenological stride frequency-stride length relation, such a solution fits the experimentally observed horizontal and vertical velocities of the body's centre of mass as a function of time in the midstance and ter-

minal stance phases for different gaits, from slow to fast walking.

(*iii*) The classical Alexander's model of human walking, which consists of a free inverted pendulum, does not reproduce the experimentally observed vertical ground reaction forces. On the other hand, we have shown that the introduction of quartic step-angle dependent muscle force along the pendulum allows the "forced" IP model to fit, rather well, the observed ground reaction forces in the mid-stance and terminal stance phases in slow, regular, and fast walking.

(*iv*) Finally, we have shown that the forced inverted pendulum model, when the muscle force values are extrapolated above the walking-running transition, gives a value of the height-dependent maximum walking speed, which is compatible with the one obtained in more sophisticated three-dimensional models of human walking.

Acknowledgements

The author would like to thank the editor and two anonymous referees for constructive suggestions and comments on an earlier version of this paper.

Conflict of interest statement
The authors declare no conflict of interest.

Funding sources
There are no sources of funding to declare.

References

1. Nyakatura JA, Melo K, Horvat T, Karakasiliotis K, Allen VR, Andikfar A, Andrada E, Arnold P, Lauströer J, Hutchinson JR, Fischer MS, Ijspeert AJ. Reverse-engineering the locomotion of a stem amniote. Nature. 2019; 351-355.
2. Harrison AJ, Molloy PG, Furlong LAM. Does the McNeill Alexander model accurately predict maximum walking speed in novice and experienced race walkers? J Sport Health Sci. 2018; 7: 372-377.
3. Lu TW, Chang CF. Biomechanics of human movement and its clinical applications. Kaohsiung J Med Sci. 2012; 28: S13-S25.
4. Racic V, Pavic A, Brownjohn JMW. Experimental identification and analytical modelling of human walking forces: Literature review. J Sound Vib. 2009; 326: 1-49.
5. Weyand PG, Smith BR, Puyau MR, Butte NF. The mass-specific energy cost of human walking is set by stature. J Exp Biol. 2010; 213: 3972-3979.
6. Massaad F, Lejeune TM, Detrembleur C. The up and down bobbing of human walking: a compromise between muscle work and efficiency. J Physiol. 2007; 582(2): 789–799.
7. Faraji S, Wu AR, Ijspeert AJ. A simple model of mechanical effects to estimate metabolic cost of human walking. Sci Rep. 2018; 8: 10998.
8. Marshall AE. A Dynamical Model for the Stride in Human Walking. Math Model. 1983; 4: 391-415.
9. Alexander RMcN. Mechanics and Scaling of Terrestrial Locomotion. In Scale Effects in Animal Locomotion, Pedley TJ, ed., pp. 93-110, Academic Press, London; 1977.
10. Saunders J, Inman V, Eberhart H. The major determinants in normal and pathological gait. J Bone Jt Surg. 1953; 35A: 543-58.
11. Geyer H, Seyfarth A, Blickhan R. Compliant leg behaviour explains basic dynamics of walking and running. Proceedings of the Royal Society B: Biological Sciences. 2006; 273(1603): 2861–2867.
12. Whittington BR, Thelen DG. A simple mass-spring model with roller feet can induce the ground reactions observed in human walking. J Biomech Eng. (2009); 131(1): 011013.
13. Lee M, Kim S, Park S. Resonance-based oscillations could describe human gait mechanics under various loading conditions. J Biomech. 2014; 44(1): 319–322.
14. Martin AE, Schmiedeler JP. Predicting human walking gaits with a simple planar model. J Biomech. 2014; 47(6): 1416–1421.
15. Li T, Li Q, Liu T. An actuated dissipative spring-mass walking model: predicting human-like ground reaction forces and the effects of model parameters. J Biomech. 2019; 90: 58–64.
16. Antoniak G, Biswas T, Cortes N, Sikdar S, Chun C, Bhandawat V. Spring-loaded inverted pendulum goes through two contraction-extension cycles during the single support phase of walking. Biol Open. 2019; 8(6): bio043695.
17. Kim S, Park S. Leg stiffness increases with speed to modulate gait frequency and propulsion energy. J Biomech. 2011; 44: 1253-8.
18. McGrath M, Howard D, Baker R. The strengths and weaknesses of inverted pendulum models of human walking. Gait Posture. 2015; 41(2): 389-94.
19. Lim H, Park S. Kinematics of lower limbs during walking are emulated by springy walking model with a compliantly connected, off-centered curvy foot. J Biomech. 2018; 71: 119–126.
20. Kuo AD. The six determinants of gait and the inverted pendulum analogy: A dynamic walking perspective. Human Movement Science. 2007; 26: 617-56.
21. Donelan JM, Kram R, Kuo AD. Mechanical work for step-to-step transitions is a major determinant of the metabolic cost of human walking. J Exp Biol. 2002; 205: 3717-27.
22. Kuo AD, Donelan JM, Ruina A. Energetic consequences of walking like an inverted pendulum: step-to-step transitions. Exerc Sport Sci Rev. 2005; 33: 88-97.
23. Koolen T, Boer TD, Rebula J, Goswami A, Pratt J. Capturability-based analysis and control of legged locomotion, Part 1: Theory and application to three simple gait models. Int J Rob Res. 2012; 31: 1094-113.

24. Hong H, Kim S, Kim C, Lee S, Park S. Spring-like gait mechanics observed during walking in both young and older adults. J Biomech. 2013; 46: 77-82.
25. Kuo AD, Stabilization of lateral motion in passive dynamic walking. Int J Robot Res. 1999; 18(9): 917–930.
26. Roos PE, Dingwell JB. Influence of simulated neuromuscular noise on movement variability and fall risk in a 3D dynamic walking model. J Biomech. 2010: 43(15): 2929–2935.
27. Englsberger J, Ott C, Albu-Schäffer A. Three-dimensional bipedal walking control using divergent component of motion. Proceedings of 2013 IEEE/RSJ International Conference on Intelligent Robots and Systems, Tokyo, Japan 2013: 2600–2607.
28. D. García-Vallejo D, Schiehlen W. 3D-simulation of human walking by parameter optimization. Arch Appl Mech 2012; 82(4): 533–556.
29. Yang QS, Qin JW, Law SS. A three-dimensional human walking model. J Sound Vib. 2015; 357: 437–456.
30. Liang H, Xie W, Zhang Z, Wei P, Cui C. A Three-Dimensional Mass-Spring Walking Model Could Describe The Ground Reaction Forces. Mathematical Problems in Engineering. 2021; 2021: 1-20.
31. Anderson FC, Pandy MG. Individual muscle contributions to support in normal walking. Gait Posture. 2003; 17: 159-69.
32. Buczek FL, Cooney KM, Walker MR, Rainbow MJ, Concha MC, Sanders JO. Performance of an inverted pendulum model directly applied to normal human gait. Clin Biomech. 2006; 21: 288-96.
33. Ellis RG, Sumner BJ, Kram R. Muscle contributions to propulsion and braking during walking and running: Insight from external force perturbations. Gait Posture. 2014; 40: 594-599.
34. Davidovits P. Physics in Biology and Medicine. 5th ed. London (UK): Academic Press; 2019.
35. Danion F, Varraine E, Bonnard M, Pailhous J. Stride variability in human gait: the effect of stride frequency and stride length. Gait Posture. 2003; 18: 69-77.
36. Alexander RMcN. The gaits of bipedal and quadrupedal animals. Int J Robot Res. 1984; 3: 49-59.
37. Turvey MT, Holt KG, Lafiandra ME, Fonseca ST. Can the Transitions to a from Running and the Metabolic Cost of Running Be Determined from the Kinetic Energy of Running? J Mot Behav. 1999; 31(3): 265-78.
38. Hanna A, Abernethy B, Neal Robert J, Burgess-Limerick R. Triggers for the Transitions Between Human Walking and Running. In Energetics of Human Activity. Sparrow W (ed). USA: Human Kinetics; 2000: 124-64.
39. Raynor AJ, Yi CJ, Abernethy B, Jong QJ. Are transitions in human gait determined by mechanical, kinetic or energetic factors? Hum Mov Sci. 2002; 21(5-6): 785-805.
40. Prilutsky BI, Gregor RJ. Swing- and support-related muscle actions differently trigger human walk-run and run-walk transitions. J Exp Biol. 2001; 204(13): 2277-87.
41. Hreljac A, Imamura RT, Escamilla RF, Edward WB. When does a gait transition occur during human locomotion? J Sports Sci Med. 2007; 6: 36-43.
42. Abramowitz M, Stegun, IA (eds). Handbook of Mathematical Functions with Formulas, Graphs, and Mathematical Tables. New York: Dover Publications; 1972.
43. Winter DA. Biomechanics of Human Movement: John Wiley Sons, Inc.; 1979.
44. Winter DA. The biomechanics and motor control of human gait: Normal, Elderly and Pathological. 2nd ed. Waterloo: Waterloo Biomechanics; 1991.
45. Patnaik L, Umanand L. Physical constraints, fundamental limits, and optimal locus of operating points for an inverted pendulum based actuated dynamic walker. Bioinspir Biomim. 2015; 10: 064001.